



(LTR)

Report No. LO-00-79-108

Date: February 8, 1980

RELEASED BY LOFT CDOS *SH*

USNRC-P-394

cy-1

**MASTER COPY**  
**DOES NOT CIRCULATE**  
**INTERNAL TECHNICAL REPORT**

**LOAN COPY**

THIS REPORT MAY BE RECALLED  
AFTER TWO WEEKS. PLEASE  
TURN PROMPTLY TO:

**NEL TECHNICAL LIBRARY**

Title: **AN EVALUATION OF THE PBF LOFT LEAD ROD TEST  
RESULTS CONCERNING SURFACE THERMOCOUPLE PERTURBATION  
EFFECTS**

Organization: **LOFT EXPERIMENTAL PROGRAM DIVISION**

*R. Hansen 2-11-88*

WAV 0 5 10031

Does not contain Export Controlled information
Author: M. J. Carboneau/E. L. Tolman
Export Control Review Number: 96168
Date of Review: 8/22/81
Reviewer Initials: <i>AS</i>

Does not contain Export Controlled information
Author: M. J. Carboneau/E. L. Tolman
Export Control Review Number: 96168
Date of Review: 8/22/81
Reviewer Initials: <i>AS</i>

Checked By: S. A. Naff

Approved By: L. P. Leach

*RECEIVED  
EG&G Idaho, Inc.  
FEB 14 1980  
INEL  
TECHNICAL LIBRARY*

THIS DOCUMENT HAS NOT RECEIVED PATENT  
CLEARANCE AND IS NOT TO BE TRANSMITTED  
TO THE PUBLIC DOMAIN





Idaho, Inc.

LOFT TECHNICAL REPORT  
LOFT PROGRAMFORM EG&G-220  
(Rev. 06-79)

TITLE		An Evaluation of the PBF LOFT Lead Rod Test Results Concerning Surface Thermocouple Perturbation Effects	REPORT NO. LTR-LO-00-79-108
AUTHOR	M. L. Carboneau/E. L. Tolman		Charge Number 52DFL0901
PERFORMING ORGANIZATION	LOFT Experiment Program Division		DATE RELEASED BY LOFT CDDCS
LOFT APPROVAL	<i>L. P. Leach (sw) S. P. Sleath</i>		February 8, 1980 <i>SL</i>

LEPD Mgr.

It is the purpose of the attached document to review and evaluate the data from the Power Burst Facility (PBF) Loss-of-Fluid Test (LOFT) Lead Rod (LLR) experiments concerning the existence or non-existence of surface thermocouple effects. Although the LLR experiments were not explicitly designed to evaluate cladding thermocouple perturbation phenomena, linear variable differential transformers (LVDTs) attached to the fuel rods provided an alternate means of evaluating the fuel rod behavior during blowdown and reflood events. In addition, several tests were performed with a rod equipped with a LVDT but no surface cladding thermocouples. This afforded an opportunity to compare the response of rods with and without cladding thermocouples by studying the LVDT data for each rod.

A systematic review is presented of the PBF LLR tests LLR-03, -05, -04, and -04A concerning possible thermocouple influences on the time-to-CHF and the time-to-quench behavior of the fuel rods. An interpretation of the data will be presented when feasible.

Furthermore, since an evaluation of the LVDT data is crucial to understanding the fuel cladding behavior and the corresponding response of the surface cladding thermocouples, appendices to this document review and analyze the LVDT data in detail.

DISPOSITION OF RECOMMENDATIONS

No disposition required.



ABSTRACT

The purpose of the PBF LOFT Lead Rod (LLR) Test program was to provide experimental data to characterize the mechanical behavior of LOFT type nuclear fuel rods under loss of coolant accident (LOCA) conditions, simulating the test conditions expected for the LOFT Power Ascension (L2) Test series.

Although the LLR tests were not explicitly designed to evaluate cladding surface thermocouple perturbation effects, comparison of the Linear Variable Differential Transformer (LVDT) data for rods instrumented with and without cladding thermocouples provided pertinent information concerning the effects of cladding thermocouples on the time to DNB and time to quench data. Documentation and review of this data is presented in the following report. It will be shown that most of the LLR data indicate that the cladding surface thermocouples did not enhance the rewetting characteristics of the rods they are attached to, even though other evidence shows that the surface clad thermocouples did quench early.

Finally, in order to accurately interpret and understand the limitations of the LVDT instrumentation, upon which thermocouple perturbation effects were evaluated, an analysis of the LVDT data as well as a review of the atypical response events that occurred during the LLR tests are presented in appendices to this document.



SUMMARY

The LOFT Lead Rod (LLR) tests have provided valuable information concerning nuclear fuel rod behavior during Loss-of-Coolant-Experiments (LOCEs) which were intended to simulate the first planned nuclear tests in the LOFT reactor complex. The data provides information on rods instrumented with and without cladding surface thermocouples (TCs), thereby furnishing a basis for evaluating the selective cooling effects of surface thermocouples and the influence of thermocouples on rod behavior.

Estimation of the cladding elongation for each test rod, based on the Linear Variable Differential Transformer (LVDT) data, is compared with the cladding thermocouple data. Observations regarding the selective cooling or quenching characteristics of rods instrumented with surface thermocouples are summarized as follows:

- (1) The LLR test data show that surface thermocouples quench before large sections of the rod can quench. Differences between LVDT and TC quench times have varied from about 0.1, for high pressure high flooding rates, to approximately 3.8 seconds, corresponding to low pressure low flooding rates.
- (2) Cladding elongation measurements on rods with and without external thermocouples are not identical; however, general trends are consistent. As a result, non-uniform rod conditions and/or non-uniform coolant conditions may exist among the LLR test rods. Nevertheless, the LVDT data for rods instrumented with and without external clad thermocouples indicates that the TCs have no significant effect on the overall cladding quench times.



(3) From the above observations it can be concluded that the cladding thermocouples do quench somewhat earlier than that indicated by the cladding elongation measurements; however, the overall mechanical response of the rod, as indicated by the LVDT, is not significantly affected.

Because of uncertainties in some of the LLR data, and the applicability of the LLR test configuration, the above observations and inferences are not conclusive with regard to the cooling effects the cladding thermocouples may have had on the LOFT experiments. Additional experimentation is ongoing to resolve these issues.



CONTENTS

ABSTRACT. . . . .	i
SUMMARY . . . . .	ii
I. INTRODUCTION. . . . .	1
II. LLR TEST SEQUENCE, GEOMETRY, AND INITIAL TEST CONDITIONS. .	3
III. ANALYSIS METHODOLOGY. . . . .	11
IV. LLR TEST RESULTS. . . . .	13
4.1 Comparison of the LVDT and Thermocouple Reponse for LLR-03 . . . . .	13
4.2 Comparison of the LVDT and Thermocouple Response for LLR-05 . . . . .	34
4.3 Comparison of the LVDT and Thermocouple Response for LLR-04 . . . . .	54
4.4 Comparison of the LVDT and Thermocouple Response for LLR-4A . . . . .	71
V. CONCLUSIONS . . . . .	89
APPENDIX A: CORRECTION OF THE LLR LVDT DISPLACEMENT TRANSDUCER DATA FOR SHROUD ELONGATION AND TEMPERATURE EFFECTS. . . . .	91
I. INTRODUCTION. . . . .	91
1.1 LVDT Theory and Operation Information. . . . .	91
1.2 LVDT Calibration Data. . . . .	93
II. A MODEL OF THE DYNAMIC RESPONSE OF THE LVDT . . . . .	96
APPENDIX B: A REVIEW OF ATYPICAL RESPONSE EVENTS OF THE LVDT INSTRUMENTATION DURING THE LLR EXPERIMENTS. . .	111
1.1 Example #1 . . . . .	111
1.2 Example #2 . . . . .	113
1.3 Example #3 . . . . .	114
REFERENCES. . . . .	117



## FIGURES

TEST LLR-03

4.	Comparison of the thermal and mechanical response of fuel rod 3121. Test LLR-03. (-1 to 10 s) . . . . .	23
5.	Comparison of the thermal and mechanical response of fuel rod 3122. Test LLR-03. (-1 to 10 s) . . . . .	24
6.	Comparison of the thermal and mechanical response of fuel rod 3123. Test LLR-03. (-1 to 10 s) . . . . .	25
7.	Comparison of the thermal and mechanical response of fuel rod 3124. Test LLR-03. (-1 to 10 s) . . . . .	26
8A.	Comparison of the thermal and mechanical response of fuel rod 3121. Test LLR-03. (0 to 50 s) . . . . .	27
8B.	An overlay showing the system pressure and the upper and lower volumetric flow rates for rod 3121. Test LLR-03. (0 to 50 s) . . . . .	27
9A.	Comparison of the thermal and mechanical response of fuel rod 3122. Test LLR-03. (0 to 50 s) . . . . .	28
9B.	An overlay showing the system pressure and the upper and lower volumetric flow rates for rod 3122. Test LLR-03. (0 to 50 s) . . . . .	28
10A.	Comparison of the thermal and mechanical response of fuel rod 3123. Test LLR-03. (0 to 50 s) . . . . .	29

10B. An overlay showing the system pressure and the upper and lower volumetric flow rates for rod 3123. Test LLR-03. (0 to 50 s) . . . . .	29
11A. Comparison of the thermal and mechanical response of fuel rod 3124. Test LLR-03. (0 to 50 s) . . . . .	30
11B. An overlay showing the system pressure and the upper and lower volumetric flow rates for rod 3124. Test LLR-03. (0 to 50 s) . . . . .	30
12. An overlay showing the mechanical response of rods 3121, 3122, 3123, and 3124. Test LLR-03. (0 to 50 s) . . . . .	31
13. An overlay showing the thermal response of rods 3121, 3122, 3123, and 3124, as determined by thermocouples located at 180° azimuthal orientation. Test LLR-03. (0 to 50 s) . . . . .	32
14. An overlay showing the thermal response of rods 3121, 3122, 3123, and 3124, as determined by thermocouples located at 0° azimuthal orientation. Test LLR-03. (0 to 50 s) . . . . .	33

#### TEST LLR-05

15. Comparison of the thermal and mechanical response of fuel rod 3121. Test LLR-05. (-5 to 20 s) . . . . .	40
16. Comparison of the thermal and mechanical response of fuel rod 3122. Test LLR-05. (-5 to 20 s) . . . . .	41
17. Comparison of the thermal and mechanical response of fuel rod 3451. Test LLR-05. (-5 to 20 s) . . . . .	42
18. The mechanical response of fuel rod 3452. Test LLR-05. (-5 to 20 s) . . . . .	43
19A. Comparison of the thermal and mechanical response of fuel rod 3121. Test LLR-05. (0 to 260 s) . . . . .	44
19B. An overlay showing the system pressure and the upper and lower volumetric flow rates for rod 3121. Test LLR-05. (0 to 260 s) . . . . .	44

20A. Comparison of the thermal and mechanical response of fuel rod 3122. Test LLR-05. (0 to 260 s) . . . . .	45
20B. An overlay showing the system pressure and the upper and lower volumetric flow rates for rod 3122. Test LLR-05. (0 to 260 s) . . . . .	45
21A. Comparison of the thermal and mechanical response of fuel rod 3451. Test LLR-05. (0 to 260 s) . . . . .	46
21B. An overlay showing the system pressure and the upper and lower volumetric flow rates for rod 3451. Test LLR-05. (0 to 260 s) . . . . .	46
22A. The mechanical response of rod 3452. Test LLR-05 (0 to 260 s) . . . . .	47
22B. An overlay showing the system pressure and the upper and lower volumetric flow rates for rod 3452. Test LLR-05. (0 to 260 s) . . . . .	47
23. Comparison of the thermal and mechanical response of fuel rod 3121. Test LLR-05. (150 to 250 s) . . . . .	48
24. Comparison of the thermal and mechanical response of fuel rod 3122. Test LLR-05. (150 to 250 s) . . . . .	49
25. Comparison of the thermal and mechanical response of fuel rod 3451. Test LLR-05. (150 to 250 s) . . . . .	50
26. The mechanical response of rod 3452. Test LLR-05. (150 to 250 s) . . . . .	51
27. An overlay showing the mechanical response of rods 3121, 3122, 3451, and 3452. Test LLR-05. (0 to 260 s) . . . . .	52
28. An overlay showing the thermal response of rods 3121, 3122, 3451, and 3452, as determined by all thermocouples located on these rods. Test LLR-05. (0 to 260 s) . . . . .	53

TEST LLR-04

29. Comparison of the thermal and mechanical response of fuel rod 3121. Test LLR-04. (-1 to 10 s) . . . . .	59
---	----

30.	Comparison of the thermal and mechanical response of fuel rod 3122. Test LLR-04. (-1 to 10 s) . . . . .	60
31.	Comparison of the thermal and mechanical response of fuel rod 3451. Test LLR-04. (-1 to 10 s) . . . . .	61
32.	The mechanical response of rod 3452. Test LLR-04. (-1 to 10 s) . . . . .	62
33A.	Comparison of the thermal and mechanical response of fuel rod 3121. Test LLR-04. (-2 to 28 s) . . . . .	63
33B.	An overlay showing the system pressure and the upper and lower volumetric flow rates for rod 3121. Test LLR-04. (-2 to 28 s) . . . . .	63
34A.	Comparison of the thermal and mechanical response of fuel rod 3122. Test LLR-04. (-2 to 28 s) . . . . .	64
34B.	An overlay showing the system pressure and the upper and lower volumetric flow rates for rod 3122. Test LLR-04. (-2 to 28 s) . . . . .	64
35A.	Comparison of the thermal and mechanical response of fuel rod 3451. Test LLR-04. (-2 to 28 s) . . . . .	65
35B.	An overlay showing the system pressure and the upper and lower volumetric flow rates for rod 3451. Test LLR-04. (-2 to 28 s) . . . . .	65
36A.	The mechanical response of rod 3452. Test LLR-04 (-2 to 28 s) . . . . .	66
36B.	An overlay showing the system pressure and the upper and lower volumetric flow rates for rod 3452. Test LLR-04. (-2 to 28 s) . . . . .	66
37.	An overlay showing the thermal response of rods 3121, 3122, and 3451. Test LLR-04. (-2.5 to 10 s) . . . . .	67
38.	An overlay showing the mechanical response of rods 3121, 3122, 3451, and 3452. Test LLR-04. (-2.5 to 10 s) . . . . .	68
39.	An overlay showing the thermal response of rods 3121, 3122, and 3451 as determined by thermocouples located on these rods. Test LLR-04. (14 to 24 s) . . . . .	69

40. An overlay showing the mechanical response of rods 3121, 3122, and 3451, and 3452 as determined by corresponding LVDTs. Test LLR-04. (14 to 24 s) . . . . . 70

TEST LLR-4A

41. Comparison of the thermal and mechanical response of fuel rod 3992. Test LLR-4A. (-1 to 10 s) . . . . . 75

42. Comparison of the thermal and mechanical response of fuel rod 3122. Test LLR-4A. (-1 to 10 s) . . . . . 76

43. Comparison of the thermal and mechanical response of fuel rod 3451. Test LLR-4A. (-1 to 10 s) . . . . . 77

44. The mechanical response of fuel rod 3452. Test LLR-4A. (-1 to 10 s) . . . . . 78

45A. Comparison of the thermal and mechanical response of fuel rod 3992. Test-4A. (0 to 300 s) . . . . . 79

45B. An overlay showing the system pressure and the upper and lower volumetric flow rates for rod 3992. Test LLR-4A. (0 to 300 s) . . . . . 79

46A. Comparison of the thermal and mechanical response of fuel rod 3122. Test-4A. (0 to 300 s) . . . . . 80

46B. An overlay showing the system pressure and the upper and lower volumetric flow rates for rod 3122. Test LLR-4A. (0 to 300 s) . . . . . 80

47A. Comparison of the thermal and mechanical response of fuel rod 3451. Test LLR-4A. (0 to 300 s) . . . . . 81

47B. An overlay showing the system pressure and the upper and lower volumetric flow rates for rod 3451. Test LLR-4A. (0 to 300 s) . . . . . 81

48A. The mechanical response of fuel rod 3452. Test LLR-4A. (0 to 300 s) . . . . . 82

48B. An overlay showing the system pressure and the upper and lower volumetric flow rates for rod 3452. Test LLR-4A. (0 to 300 s) . . . . . 82

49.	An overlay showing the thermal and mechanical response of fuel rod 3992. Test LLR-4A. (230 to 250 s) . . . . .	83
50.	An overlay showing the thermal and mechanical response of fuel rod 3122. Test LLR-4A. (230 to 250 s) . . . . .	84
51.	An overlay showing the thermal and mechanical response of fuel rod 3451. Test LLR-4A. (230 to 250 s) . . . . .	85
52.	An overlay showing the thermal and mechanical response of fuel rod 3452. Test LLR-4A. (230 to 250 s) . . . . .	86
53.	An overlay showing the thermal response of rods 3992, 3122, and 3451 as determined by all cladding thermocouples. Test LLR-4A. (0 to 300 s) . . . . .	87
54.	An overlay showing the thermal response of rods 3992, 3122, 3451, and 3452 as determined by corresponding LVDTs. Test LLR-4A. (0 to 300 s) . . . . .	88

#### APPENDIX A FIGURES

A1.	Schematic of the LVDT used in the Power Burst Facility reactor. . . . .	92
A2.	Family of calibration curves for the LLR fuel rod 3122 LVDT . . . . .	103
A3.	LVDT model. . . . .	104
A4.	LVDT response and the estimated cladding displacement for rod 3121. Test LLR-03 . . . . .	105
A5.	LVDT response and the estimated cladding displacement for rod 3451. Test LLR-05 . . . . .	105
A6.	LVDT response and the estimated cladding displacement for rod 3121. Test LLR-04 . . . . .	106
A7.	LVDT response and the estimated cladding displacement for rod 3451. Test LLR-4A . . . . .	106
A8.	The estimated LVDT temperature correction factor. Based on the "inlet coolant temperature" for rod 3451. Test LLR-05. . . . .	107

A9. An overlay of the orginal LVDT data for rod 3451 and the LVDT-temperature-corrected data. Test LLR-05 . . .	107
A10. An overlay showing the LVDT data for rod 3451 and the adjusted LVDT data corrected for temperature effects and shroud elongation. Test LLR-05 . . . . .	108
A11. An overlay showing the LVDT data for rod 3451 and the adjusted LVDT data corrected for temperature effects, shroud elongation, and support tube motion. Test LLR-05 . . . . .	108
A12. An overlay showing the LVDT data for rod 3451 and the adjusted LVDT data corrected for shroud elongation. Test LLR-05 . . . . .	109
A13. An overlay showing the LVDT data for rod 3451 and the adjusted LVDT data corrected for shroud elongation and support tube elongation. Test LLR-05 . . . . .	109
A14. An overlay of the estimated cladding displacement and the average thermocouple data for rod 3451. Test LLR-05 . . . . .	110

#### APPENDIX B FIGURES

B1. Overlay of LVDTs for Test LLR-03. . . . .	115
B2. Overlay of LVDTs for Test LLR-05. . . . .	115
B3. Overlay of LVDTs for Test LLR-04. . . . .	116
B4. Fuel centerline thermocouple data for rods 3121, 3451, and 3452. Test LLR-04. . . . .	116

TABLES

1. Fuel Rod Designations and Cladding Surface Thermocouple Locations for PBF/LOFT Lead Rod Tests. . . . .	9
2. Initial Conditions for the PBF/LLR Tests Prior to Blowdown . . . . .	10
3. LLR-03. Estimated Time of Initial DNB . . . . .	15
4. LLR-03. Estimated Elongation Turnaround Time and Rod Quench Time . . . . .	19
5. LLR-05. Estimated Time of Initial DNB . . . . .	36
6. LLR-05. Estimated Elongation Turnaround Time and Rod Quench Time . . . . .	37
7. LLR-04. Estimated Time of Initial DNB . . . . .	56
8. LLR-04. Estimated Elongation Turnaround Time and Rod Quench Time . . . . .	57
9. LLR-4A. Estimated Time of Initial DNB . . . . .	73
10. LLR-4A. Estimated Elongation Turnaround Time and Rod Quench Time . . . . .	74
A1. LLR LVDT Temperature Response Data . . . . .	95

## I. INTRODUCTION

The fuel clad temperature is an essential indicator of the fuel rod response and the local thermal-hydraulic behavior in a nuclear reactor during off normal and accident conditions. The measurement of the cladding temperature during a Loss-of-Coolant-Experiment (LOCE) can be sensitive to the thermocouple rod attachment and geometry. For example, external surface clad thermocouples can influence the cladding temperature and possibly modify the thermal-hydraulic conditions surrounding the rod in such a way as to (a) selectively enhance the heat transfer characteristics from the rod (fin effect), (b) influence the rod critical heat flux (CHF), and (c) affect rod rewet and quench times. Any phenomenon that significantly influences rod behavior and can be attributed to the presence of surface clad thermocouples will be referred to as a thermocouple/rod perturbation effect.

A series of four tests, identified as LLR-03, -05, -04, and -4A (performed in this sequence), was recently completed at the Power Burst Facility (PBF). These tests were designed to investigate the thermal-mechanical behavior of LOFT type fuel rods during loss of coolant transients similar to those expected in the LOFT power ascension (L2) test series. Although the LLR tests were not explicitly designed to evaluate cladding surface thermocouple effects, linear variable differential transformers (LVDTs) attached to the fuel rods have provided an alternate means of evaluating the fuel rod behavior during blowdown and reflood events. In addition, several tests were performed with a rod equipped with a LVDT but no surface cladding thermocouples. This afforded an opportunity to compare the response of rods with and without cladding thermocouples by studying the LVDT data for each rod. It is the purpose of this report to review and evaluate the pertinent data from the LLR tests concerning the existence or nonexistence of thermocouple perturbation effects.

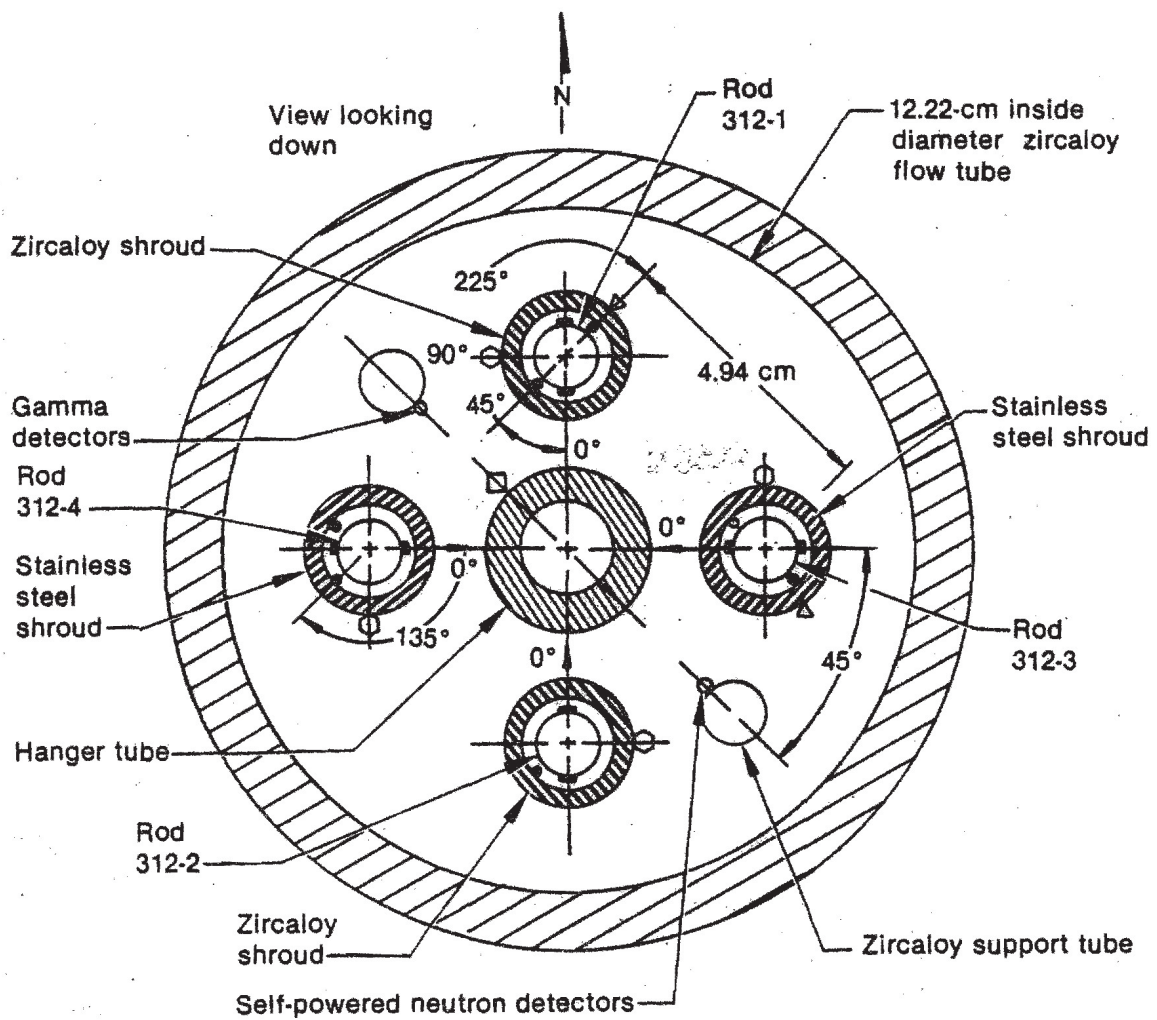
The next section of the report summarizes the LLR test sequence, test geometry, and initial test conditions. Section III describes the analysis methodology for evaluating the perturbation effects of surface cladding thermocouples. Section IV presents the test data and evaluates the DNB and quench characteristics for each of the LLR test rods in each experiment. In addition, a review of several instrument response anomalies observed during each test is addressed. Section V presents the conclusions of this report concerning the effects of thermocouples on rod behavior.

## II. LLR TEST SEQUENCE, GEOMETRY, AND INITIAL TEST CONDITIONS

A detailed discussion of the design and function of the PBF LLR test train, test program, experimental equipment, test procedure, and test predictions is presented in references (1), (2), and (3). For convenience, however, a short outline of the major features relating to the LLR test sequence, test geometry, and initial test conditions is presented below.

The LLR test series consisted of four LOCE transients, preceded by a power ramping sequence to precondition the test rods. Each of the LLR tests was performed with four separately shrouded LOFT type fuel rods. The design of the LLR fuel rods is identical with the LOFT fuel rod design with only a few exceptions. For example, the active length of the LOFT rod is 1.68 m while the LLR fuel rod is only 0.914 m long. In order to provide individual flow channels for each test rod, the LLR fuel rods are separately enclosed within a circular flow shroud. The geometric design of the LLR test assembly provides similar but not necessarily identical thermal-hydraulic conditions for each test rod. Typical test configurations for these experiments appear in Figures 1A, 1B, and 1C. Table 1 lists the thermocouple location and flow shroud material data for each test; notice that for tests 5, 4, and 4A, rod #3452 did not have surface cladding thermocouples. Table 2 summarizes the LLR initial test conditions. The valve sequencing for the LLR tests was selected to closely simulate the expected LOFT system thermal hydraulic conditions that existed during the first few seconds of the blowdown transient.

Selected fuel rods were replaced after tests LLR-03 and LLR-04. A replacement rod in tests LLR-05, -04, and -4A was unique in that no cladding external thermocouples were utilized. Figure 2 shows the rod configuration and thermocouple location for each test. Also, the peak cladding temperature for each rod is identified in Figure 2. A schematic of the PBF LLR test train installed in the PBF reactor In-Pile Tube (IPT) is illustrated in Figure 3.

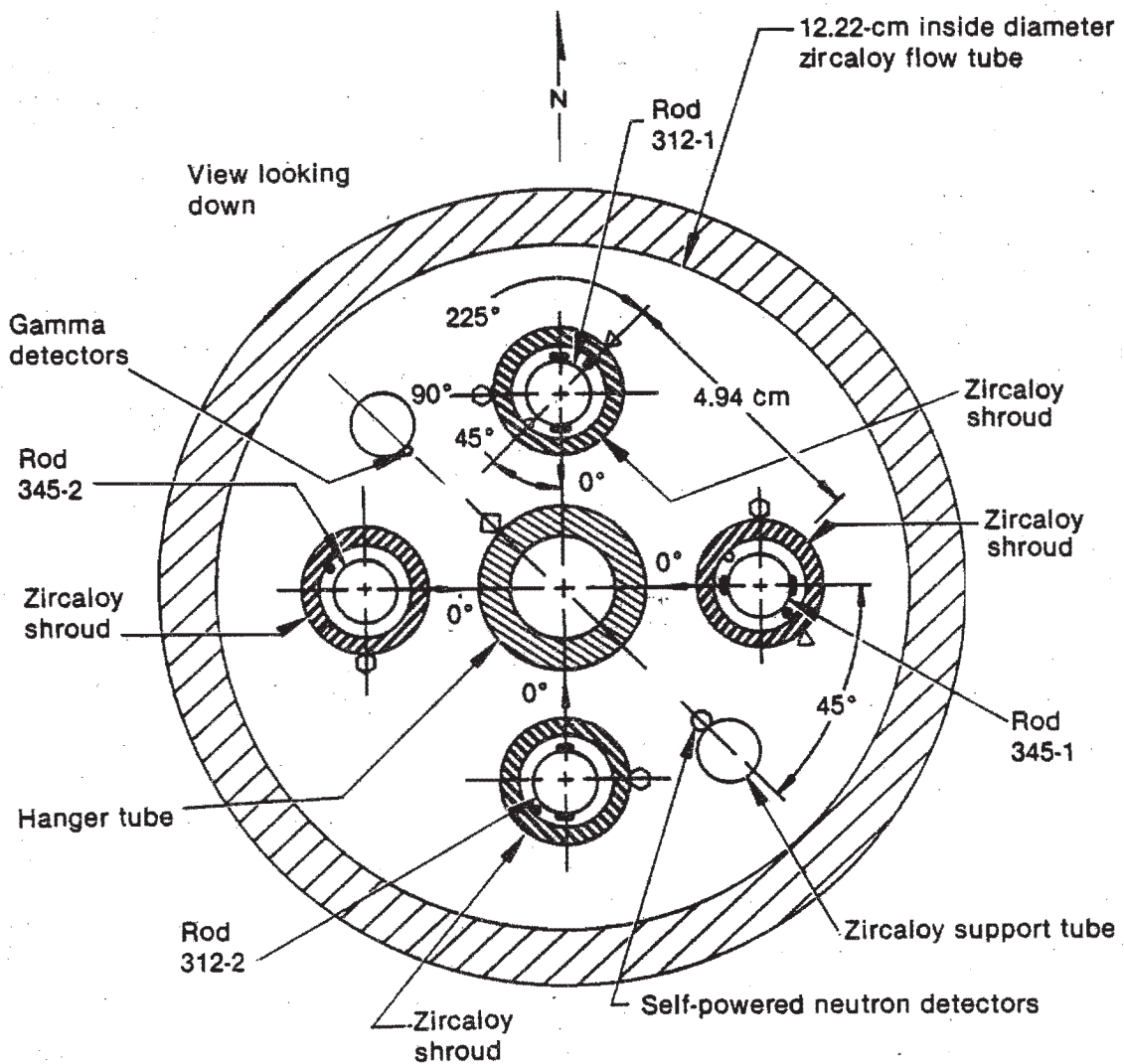


- △ 3 Outer shroud thermocouples
- 3 Midcoolant thermocouples
- Differential thermocouples
- Cladding thermocouples
- Flux wire
- Test train flux wire

All rod shrouds have inlet and outlet thermocouples located at the 45° azimuthal location inside the shroud

INEL-A-12 785

Fig. 1A Test fuel rod instrumentation schematic. Test LLR-03.

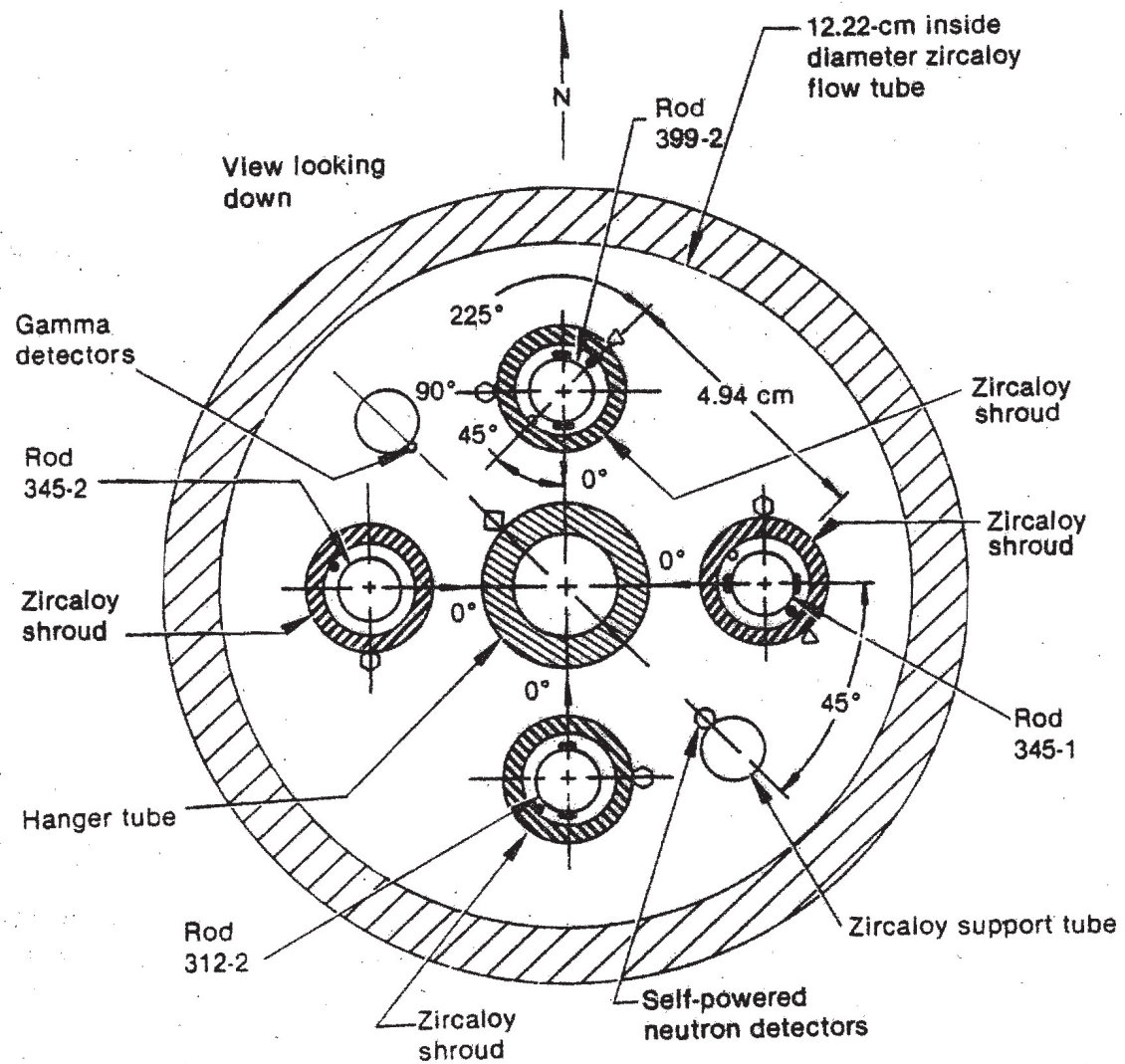


- △ 3 Outer shroud thermocouples
- 3 Midcoolant thermocouples
- Differential thermocouples
- Cladding thermocouples
- Flux wire
- Test train flux wire

All rod shrouds have inlet and outlet thermocouples located at the 45° azimuthal location inside the shroud.

INEL-A-12 786-1

Fig. 1B Test fuel rod instrumentation schematic. Tests LLR-04 and LLR-05.



- △ 3 Outer shroud thermocouples
- 3 Midcoolant thermocouples
- Differential thermocouples
- Cladding thermocouples
- Flux wire
- Test train flux wire

All rod shrouds have inlet and outlet thermocouples located at the 45° azimuthal location inside the shroud.

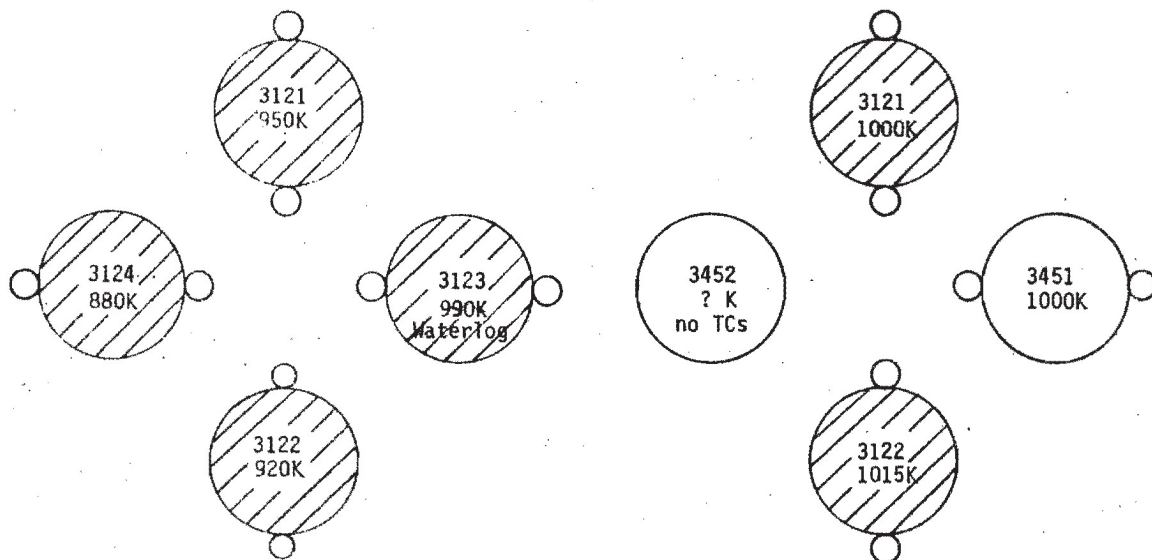
INEL-A-12 770

Fig. 1C Test fuel rod instrumentation schematic. Test LLR-4A.

LLR-03

LLR-05

LTR L0-00-79-108



LLR-04

LLR-4A

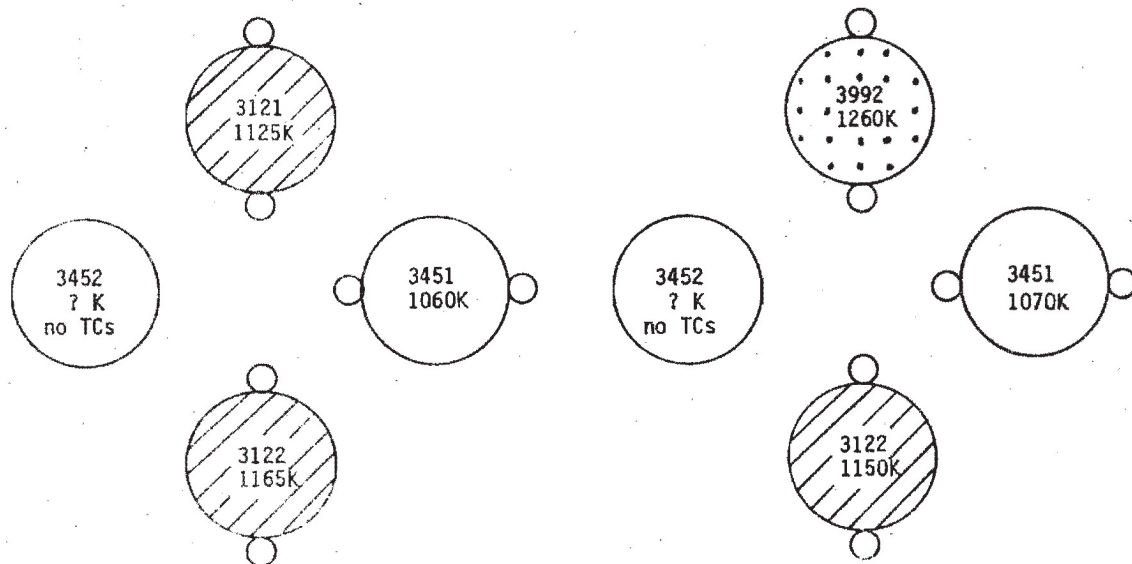


Fig. 2. Test schematic and peak measured surface temperature.

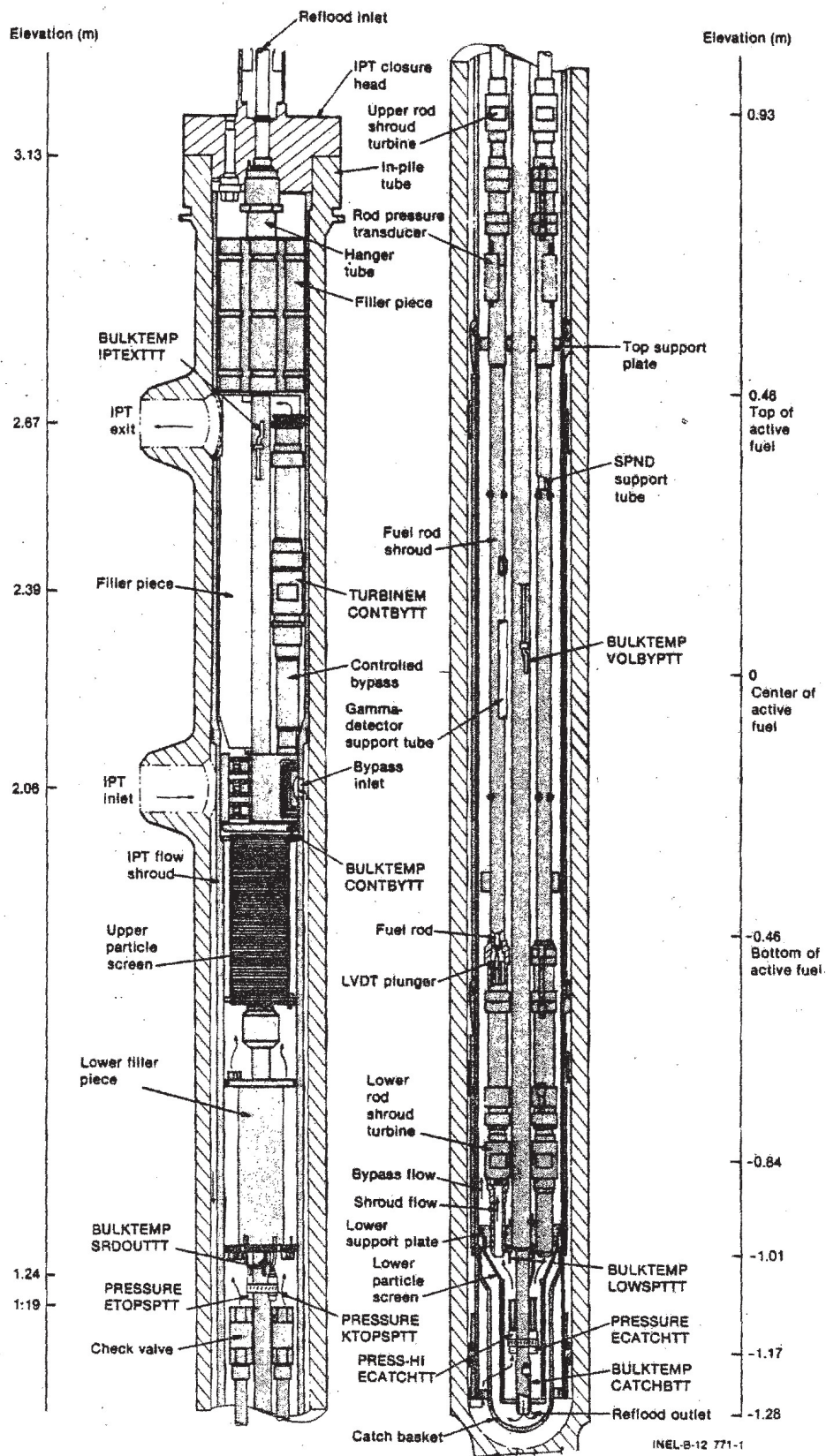


Fig. 3 LLR test train drawing.

TABLE 1

FUEL ROD DESIGNATIONS AND CLADDING SURFACE THERMOCOUPLE LOCATIONS  
FOR PBF/LOFT LEAD ROD TESTS

Rod	Number	Tests	LLR-	Shroud	*Thermocouple Location (m)		
					Clad T/C #1	Clad T/C #2	Centerline
					180°	0°	
1	312-1	3,4,5	Zirc	Zirc	0.533	0.533	0.533
2	312-2	3,4,5,4A	Zirc	Zirc	0.533	0.457	0.457
3	312-3	3	SS	SS	0.533	0.533	0.533
4	312-4	3	SS	SS	0.533	0.533	0.533
5	345-1	4,5,4A	Zirc	Zirc	0.533	0.533	0.533
6	345-2	4,5,4A	Zirc	Zirc	-	-	0.457
7	399-1	Spare	Zirc	Zirc	0.533	0.457	0.457
8	399-2	4A	Zirc	Zirc	0.457	0.314	0.457

\* From bottom of active fuel.  
All rods were unpressurized (0.1034 MPa, 15 psia).

TABLE 2

INITIAL CONDITIONS FOR THE PBF/LLR TESTS PRIOR TO BLOWDOWN<sup>a</sup>

Test	Reactor Power (MW)	MLHGR (kW/m)	System Pressure (MPa)	IPT Inlet temperature	Average Core Differential temperature	Individual Shroud Flow 1/s	Controlled Bypass Flow 1/s	Total IPT Flow 1/s
LLR -3	14.52	40.5	15.57	595.0	11.07	0.585	6.08	9.13
LLR -5	14.52	47.4	15.5	603.4	10.46	0.60	6.68	9.35
LLR -4	19.3	56.6	15.6	600.0	10.11	0.80	8.71	12.4
LLR -4A	19.3	55.6	15.5	600.0	11.5	0.78		

a. Measurement determination and location identified in References (2 and 3).

## III. ANALYSIS METHODOLOGY

There are two principal techniques that will be used to analyze the PBF LLR data for possible thermocouple perturbation effects. First, for a given set of thermal-hydraulic boundary conditions, thermocouple effects can be investigated by comparing the cladding elongation response of fuel rods instrumented with and without surface clad thermocouples. Since the LLR tests 5, 4, and 4A contained rods with and without surface cladding thermocouples (note Table 1), and since all rods were instrumented with linear variable differential transformers (LVDTs) and centerline fuel thermocouples, an assessment of the thermocouple effects on fuel rod response can be made by comparing the cladding elongation and centerline temperature data. For instance, if significant differences exist between the LVDT data for rods with and without surface thermocouples, for a given test, then the possibility of a thermocouple perturbation effect would have to be seriously considered, as long as the thermocouple attachment integrity was not in question, and the thermal-hydraulic conditions existing between the comparison flow channels are the same.

The second technique that will be considered involves the comparison of LVDT data and surface thermocouple data for any one particular rod during each test. The advantage of this technique over the previous method is that the assumption of identical thermal-hydraulic conditions between separate flow channels is not necessary. However, in either case the principal disadvantage of using LVDTs to evaluate fuel rod behavior and inferring information about thermocouple effects is that the LVDTs measure the integral rod response and therefore can only project average conditions along any given rod, whereas thermocouples represent a discrete measurement and hence infer information for only one particular point on the rod. In general, the response of a given section of the fuel rod, say near a thermocouple, may not represent a typical condition existing along the

entire length of the rod, as indicated by the LVDT. For instance, thermal hydraulic conditions can have an axial dependency along the length of the fuel rod, particularly during rod rewet events, as was shown by the axial dependent thermocouple response during the LOFT L2-2 and L2-3 experiments. Consequently, it is possible that a local rewet event or precursory cooling phenomenon, not caused by a surface clad thermocouple, might occur at particular locations on the fuel rod surface where it could be detected by a thermocouple located near the phenomenon, while the LVDT instrumentation indicating the overall elongation of the rod may not indicate an abrupt change. An event of this nature might be incorrectly interrupted as a thermocouple perturbation effect when indeed the phenomenon has no relevant association with surface cladding thermocouples. Hence, one has to be careful not to infer conclusions based on only a few isolated events. Rather, the best that can be hoped for is to evaluate all the data and draw conclusions based on the evidence supported by an overwhelming collection of the data.

## IV. LLR TEST RESULTS

4.1 Comparison of the LVDT and TC Responses for LLR-03

As shown in Figure 1A the fuel rods used in the LLR-03 test were designated as 3121, 3122, 3123, and 3124. For the LLR-03 test, rods 3121 and 3122 were encased in zircaloy-4 flow shrouds, and rods 3123 and 3124 were encased in stainless steel flow shrouds. The different shroud materials caused a power tilt of 0.87/1.0 for the stainless steel (or low power rods) and the zircaloy shrouded (or high power) rods.<sup>2</sup> The power tilt was designed to simulate the different power characteristics of the peripheral and central rods in the LOFT core. During the LLR-03 test, however, rod 3123 developed a leak, became waterlogged, and later failed during the blowdown. Consequently, an accurate interpretation of the test data for rod 3123 is difficult. After completion of the LLR-03 experiment, the stainless steel shrouded rods were replaced with zircaloy shrouded rods. Therefore, for tests LLR-05, -04, and -4A, all test rods experienced similar power conditions.

Figures 4 through 11 compare the response of the cladding thermocouples and LVDT data for each of the LLR-03 fuel rods 3121, 3122, 3123, and 3124 for time intervals of -1 to 10 and 0 to 50 seconds. Figures 8B, 9B, 10B, and 11B display the system pressure and hydraulic data (i.e., turbine measurements of the volumetric flow rates) for each test rod in LLR-03. This data can be directly compared with the LVDT and cladding thermocouple data in Figures 8A through 11A, respectively. Figure 12 shows an overlay of the responses of the four LVDTs and Figures 13 and 14 show overlays of the thermocouple data. The events of particular importance that will be discussed with regard to thermocouple perturbation effects are the time to DNB (departure from nucleate boiling) and rod quench indicated by these figures. An interpretation of the data will be presented when feasible.

The data displayed in Figures 4, 5, 6, and 7 illustrate the rod DNB during the early portion of the blowdown. Here, the saturation temperature curve (not shown in these figures) and the coolant temperature data, taken at the outlet of the flow channel are nearly identical. Consequently, an estimate of the cladding temperature departure time from saturation conditions, indicating DNB, can be made relative to the displayed coolant temperature data. Also, an estimate of DNB can be made from the LVDT data. These estimates are collected in Table 3.

All of the data in Table 3, except for one point, suggest that the LVDT detects an earlier time for DNB than that determined by the surface clad thermocouples. In symbols, this could be written as

$$t_{\text{LVDT}}^{\text{DNB}} \leq t_{\text{TC}}^{\text{DNB}} \quad (1)$$

Two possible reasons for this correlation are discussed below.

Since DNB conditions are attained at different times for different axial locations along the rod, one reasonable hypothesis for explaining the early DNB response of the LVDT rests on the assumption that the LVDT instrumentation can detect the first localized film boiling event occurring at some location along the length of the rod. Meanwhile, the surface thermocouples, representing a point measurement, can only indicate the time when the neighboring clad surface experiences DNB. Consequently, the time to DNB as determined by the LVDT should be less than or equal to that determined by the TCs. The only time when the two quantities should be equal would be when the initial DNB condition occurs near enough to a thermocouple junction to be detected simultaneous with the LVDT response. The single inconsistency in the early LVDT/DNB theory occurred on the high power rod 3121. As is evident from Figure 4, the LVDT on this rod indicated a later DNB time than the surface clad thermocouple located at 0° azimuthal orientation

TABLE 3

LLR-03

## ESTIMATED TIME OF INITIAL DNB

Instrument	Rod Number			
	3121	3122	3123*	3124
LVDT	2.8	2.0	2.0	1.8
TC 180° 0.533 m	2.8	4.5	2.5	2.4
TC 0° 0.533 m	2.4		2.5	2.4
TC 0° 0.457 m		2.6		

The above numbers indicate the approximate time (in seconds) during blowdown that the rod temperature significantly deviates from the saturation temperature, indicating DNB, as determined from the given instrumentation. Interpretation of the data, especially the LVDT data, with regard to the initiation of DNB is somewhat subject and might be open to alternative evaluations.

Numbers reported in the above table have been suggested by PBF personnel<sup>15</sup>.

\* Rod 3123 failed at 12.3 seconds into the blowdown transient. The rod failure resulted from a water-log condition that existed prior to blowdown.

and 0.533 m from the bottom of the rod. It has been suggested<sup>4</sup> that this discrepancy may be due to a timing offset error in the LVDT data because it is not likely that the high power rod 3121 experienced DNB, as determined by the LVDT, later than the low power rods 3123 and 3124.

Although the above hypothesis explains the early LVDT DNB data and does not involve thermocouple perturbation effects, there is another hypothesis that is also possible, explains the data, and is directly linked to surface thermocouple cooling phenomena, i.e., "fin effects." To begin, it is possible to look at Figures 4 through 7 and say that the "delayed" response in the thermocouple DNB data relative to the LVDT data, and sometimes the wide discrepancies between oppositely positioned thermocouples, suggests that selective cooling effects are taking place near the thermocouples and thereby "delaying" DNB at these places while other more remote sections of the rod are experiencing film boiling, as shown by the LVDT data. This can occur because thermocouple sheaths extend only down to about the core midplane and consequently the lower half of the rod may be experiencing DNB while the upper section with "fin" TCs may be cooling the cladding surface and thereby delaying DNB. Whether or not this is true cannot be determined from the presently available data for a variety of reasons: (a) the thermal response of the rod at other axial positions is not known, (b) the hydraulic conditions between flow channels may be non-uniform, (c) a comparison response for rods without external surface clad thermocouples is not possible for this test, and (d) the response of rods with full length TC/rod sheaths is not known.

The presently available data are simply not sufficient to decide between the above two theories or even alternate interpretations of the LVDT and thermocouple data. The strongest statement that can presently be made about the first 10 seconds of the LLR-03 data is that the LVDT generally leads the response of the thermocouples in

determining the time to DNB, and that this may result from either thermocouple "fin" effects or axially dependent DNB conditions not dependent on cladding thermocouples.

There is one final observation that should be made. Notice that in Figure 5 there is a significant delay in the response of the thermocouple located at 0.533 m and 180° compared with the TC at 0°. As will be seen in some later tests this same thermocouple also behaves in a rather atypical fashion. One conceivable explanation for this thermocouple response anomaly involves the possibility of a thermocouple attachment problem. If for any reason the sensitive junction of the TC is perturbed from its intended position, then the thermocouple may not accurately measure the cladding temperature. Furthermore, the TC attachment geometry can vary slightly from test to test, due to rod power changes, cycling effects, and other factors. In the above case, it is possible that the TC junction is slightly farther away from the cladding surface than the other TCs. Consequently, the TC might be cooler than the clad and therefore enters into DNB at a later time than the cladding surface, as indicated by the other thermocouples. This explanation appears to explain other anomalies in later tests; however, not all of the test data are consistent. Other theories including leaking check valves and rod bowing effects are also possible. Additional observations will be pointed out as the behavior of this rod is studied in the later tests.

Figures 8A, 9A, 10A, and 11A present overlay plots of the intermediate time behavior of the cladding thermocouples, cladding elongation, the outlet coolant temperature, and the midplane shroud temperature for each of the four test rods 3121, 3122, 3123, and 3124, respectively. These figures show that all rods quenched between about 36 and 40 seconds into the blowdown transient. This particular rewet was initiated by opening a hot leg blowdown valve at 22 seconds and then closing the large cold leg blowdown valve at 35 seconds,

subsequently changing the test system hydraulic resistances and thereby allowing a low quality two-phase mixture to enter the test region and rewet the rods.

By comparing the LVDT rod quench and clad elongation turnaround, with the cladding thermocouple quench and temperature turnaround data, an evaluation of possible thermocouple "fin" effects can be made during reflood. Table 4 lists estimates of the time to rod quench and turnaround times for the cladding surface thermocouples and LVDT instrumentation, as determined from Figures 8A through 11A.

Before interpreting the data in Table 4 it should be pointed out that at approximately 12.3 seconds into the transient, fuel rod 3123 ballooned and ruptured. This failure resulted from a water-logged condition that existed in the rod prior to blowdown. Consequently, it may be difficult to assess the behavior of this rod, especially during rod quench, with regard to surface clad thermocouple effects when the rod geometry and structural properties may be markedly different than non-failed rods. Nevertheless, rod rewet times have been estimated for rod 3123 and are listed in Table 4. A review of the data for rod 3123 will be presented after the behavior of the three non-failed rods has first been studied.

From Table 4 it can be seen that the cladding elongation turnaround times occur approximately 0.3 seconds after the thermocouples rewet; and the rod quench, indicated by the LVDT data, occurs even later. To present some possible explanations for this response event, the behavior of each rod during rewet will be studied and compared with the responses of the other rods.

For rod 3121 (note Figure 8A), the external thermocouple experiences a very rapid quench starting at about 36.2 seconds and ending at a relatively stable value near 37.0 seconds. Little or no precursory cooling effect is evident in the thermocouple data. In contrast, the LVDT turnaround time at 36.5 seconds suggests a

TABLE 4

LLR-03

## ESTIMATED ELONGATION TURNAROUND TIME AND ROD QUENCH TIME

Instrument	Rod Number			
	3121	3122	3123*	3124
LVDT	36.5/40.0	36.5/	36.5/	36.5/
TC 180° 0.533 m	36.2	36.2	36.0/37.5	36.2
TC 0° 0.533 m	36.2		36.0/37.5	36.2
TC 0° 0.457 m		36.2		

The first number indicates the approximate turnaround time (in seconds) for the response of the LVDT, i.e., the time of maximum rod elongation prior to rod cooldown. The second number represents the approximate rod quench time as indicated by the LVDT. A blank entry in the LVDT data indicates that a unique rod quench time could not be assessed. The temperature turnaround time and the rod quench time, as determined from the TC data, are nearly the same for non-failed rods, and are therefore reported as a single number.

---

- \* Rod 3123 failed at 12.3 seconds into the blowdown transient. The rod failure resulted from a water-log condition that existed prior to blowdown.

---

classical precursory cooling period of approximately 3.5 seconds, followed by a rapid rod quench at 40 seconds. This behavioral anomaly between the responses of the two instruments suggests that the thermocouple may have indeed selectively enhanced rod cooling effects, as supported by the precursory cooling tendency in the LVDT data, to such a point when the rod itself could rewet at 40 seconds. However, the LVDT response of this rod is different than the responses of the other rods, even though all rods experienced similar hydraulic conditions. For example, consider the response of rod 3122 in Figure 9A. Again we see the sudden thermocouple quench starting at 36.2 seconds and the LVDT turnaround time at about 36.5 seconds with a precursory cooling period evident in the LVDT data until about 40.5 seconds where the cladding elongation data has stabilized. No clearly definable quench time is evident in the LVDT data for rod 3122, as compared with rod 3121. Likewise, rod 3124 shows a corresponding turnaround time in the LVDT data near 36.5 seconds, and then decreases to a stable value at 41 seconds. Between 36.5 and 41 seconds cooling effects and perhaps local rewet events take place; however, nowhere is there evidence that the entire rod experienced such a rapid and entire rewet as seen in the data for rod 3121.

Another interesting observation can be made about the TC behavior of rods 3121, 3122, and 3124. Shortly after the thermocouples rewet, the TCs noticed a sudden and rapid increase in temperature, essentially another DNB. This is not as noticeable in Figure 8A with rod 3121 as it is evident in Figures 9A and 11A with rods 3122 and 3124 respectively. This thermocouple "flutter" behavior may be indicative of a thermocouple selective cooling effect. That is, the thermocouples being slightly cooler than the adjoining clad surface are subsequently more likely to rewet as the coolant floods the test assembly than the cladding surface. Then, as heat is transported from the clad to the thermocouple the liquid boils off the thermocouple and it experiences another DNB. This could be followed by another thermocouple rewet and possibly another DNB. This "flutter" might continue until the stored energy and/or clad temperature of the rod

permitted rewetting. During this time period the LVDT notices only a gradual decrease in the rod length, relative to the shroud, and no typical overall rewetting response, except for rod 3121 near 40 seconds. These data suggest that the TCs may be experiencing preferential rewetting conditions.

Without having discussed the response of rod 3123, the data at present suggests that no sudden overall rewet occurred at any given time for rods 3122 and 3124; but rather a time varying rewet over the axial length of the rod or possibly several very localized rewets or even rewets of extremely short duration so that the energy stored in the rods was gradually dissipated. Whether or not the external thermocouples influenced rod cooling and the rewetting behavior of the rod cannot be established with reasonable certainty. Perhaps the strongest statement that can be made so far is that the response of the thermocouples are not representing the overall response of the cladding temperature. This does not mean that the thermocouples are giving inaccurate data about the cladding temperature near the TCs, but rather the entire clad cannot be experiencing a rapid quench at 36.2 seconds, because the LVDT should have detected such an event. In other words, the local cladding surface near the TCs may be rewetting and then going into DNB as heat is transported into the region from other axial sections. Either hypothesis is possible, i.e., (a) TC rewet followed by TC DNB, or (b) clad rewet near the TC followed by a subsequent clad DNB near the TC. About the only thing that can be said with any certainty is that one cannot adequately determine fuel rod behavior with TCs located at only one axial position along the rod. Nor can one adequately compare the response of an integral type instrument, i.e., LVDT, with a single pair of thermocouples located at one axial position.

Now consider the behavior of rod 3123, shown in Figure 10A. As was mentioned before, rod 3123 failed at 12.3 seconds into the transient and interpretation of the data for this rod is somewhat questionable. Nevertheless, there are a few interesting observations

that should be pointed out. First, as in the previous cases, the LVDT response begins to turn around at about 36.5 seconds and moves downward rather quickly until at about 38.5 seconds an unexplained increase occurs. Since the data after 38.5 seconds is not fully understood, discussion of the data will be limited to the time interval between 36 and 38.5 seconds.

At about 36.0 seconds the thermocouples for rod 3123 show a temperature turnaround followed by a precursory cooling period to 36.5 seconds where they experience a rapid quench that ends at a stable temperature base at 38.5 seconds. The response of the thermocouples on this rod appear to be more representative of a non-uniform rod quench than the thermocouple data for the previous rods. The geometric distortion of the rod may have had an effect on the time to quench as indicated by the surface thermocouples. Certainly the LVDT response, preceding rod quench, was affected by the rod ballooning and failure.

A synopsis of the two theories discussed above concerning possible explanations for the behavior of the LVDTs and TCs during DNB and rod rewet events are presented below.

- (1) The thermocouples are accurately reflecting the local cladding temperature, rewet behavior, and DNB events. And the LVDT is accurately reflecting the overall (or average) fuel rod behavior. The difference between the two instrument responses is that the average behavior need not reflect the behavior of the rod at any given axial position on the rod, e.g., the TC sensitive junction.
- (2) The thermocouples are preferentially cooling the cladding surface according to fin effects. The early quench of the thermocouples for rods 3121, 3122, and 3124 suggests that because the TCs are farther from the clad surface they are

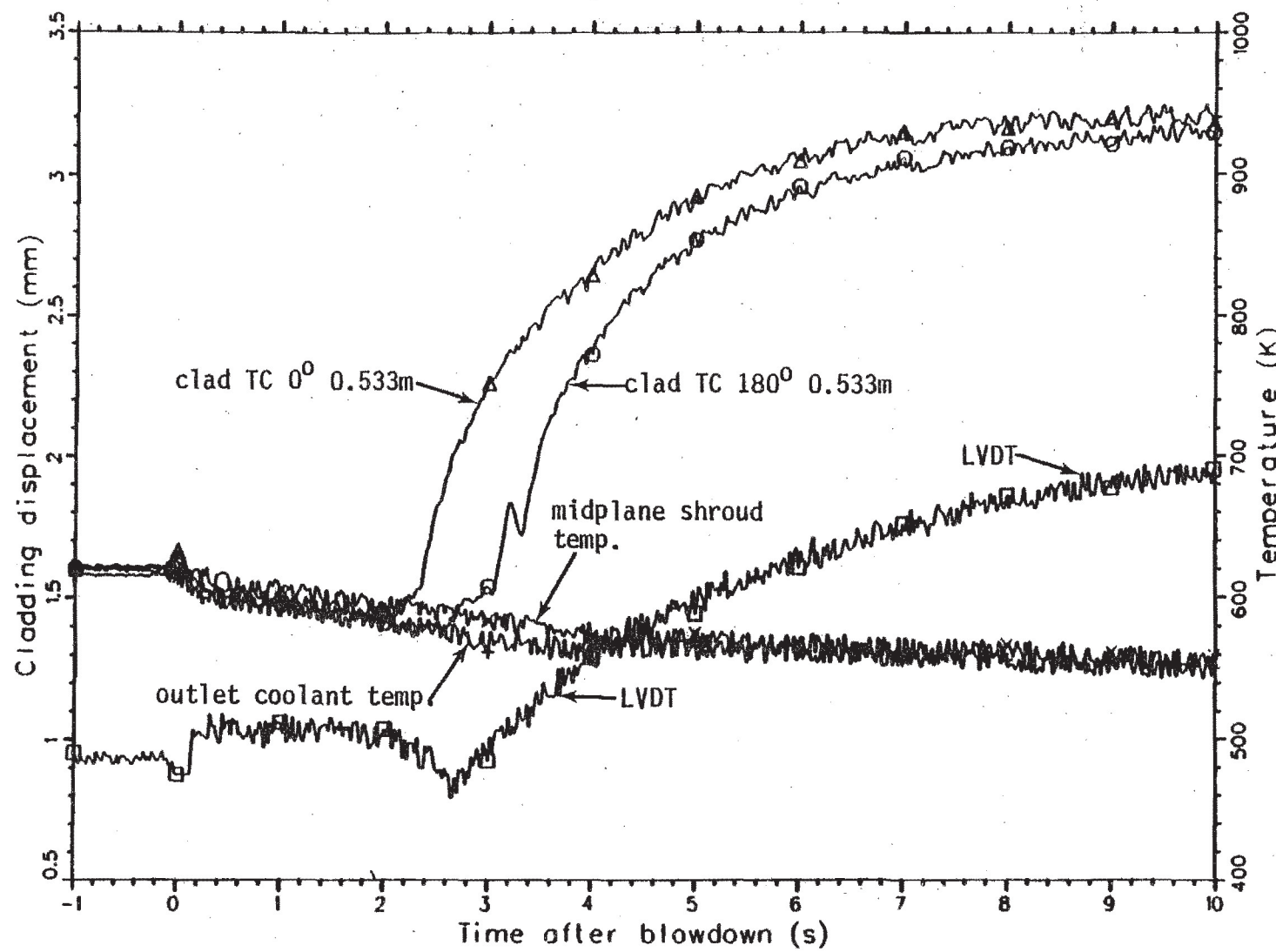


Fig. 4 Comparison of the thermal and mechanical response of fuel rod 3121. Test LLR-03.

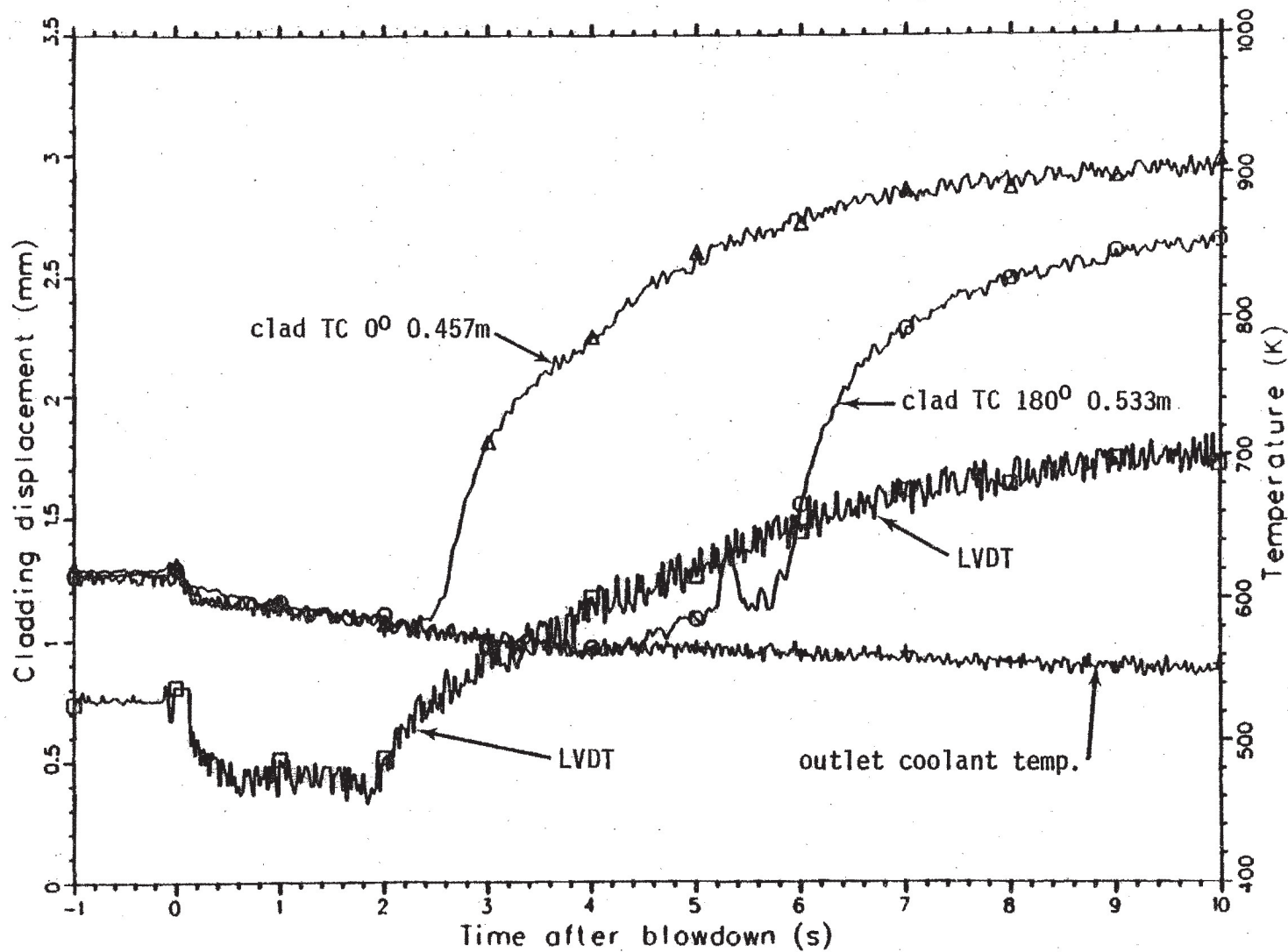


Fig. 5 Comparison of the thermal and mechanical response of fuel rod 3122. Test LLR-03.

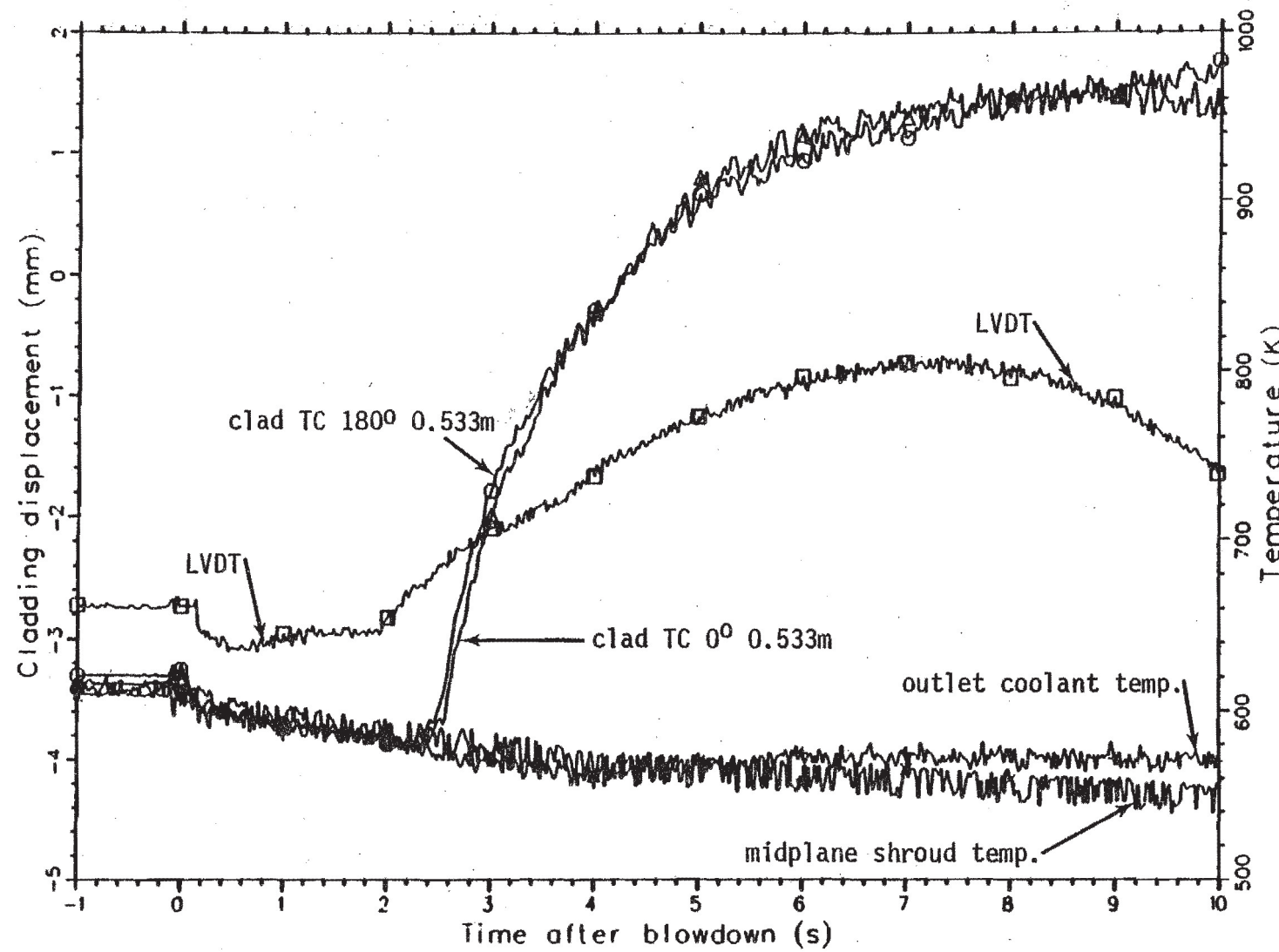


Fig. 6 Comparison of the thermal and mechanical response of fuel rod 3123. Test LLR-03.

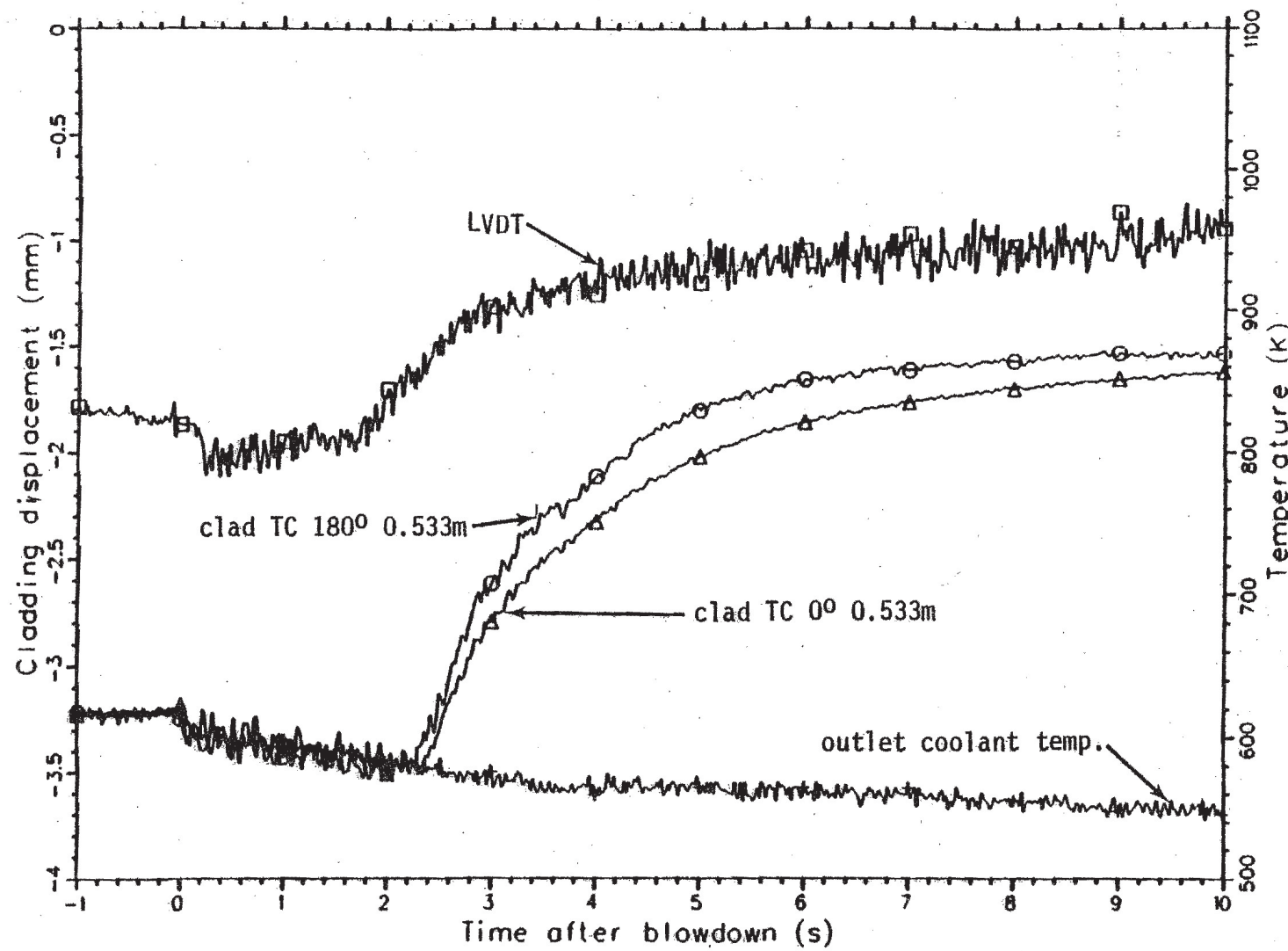


Fig. 7 Comparison of the thermal and mechanical response of fuel rod 3124. Test LLR-03.